Back-donation in High Valent d^0 Metal Complexes: Does it Exist? The case of Nb^V

Gianluca Ciancaleoni,[a] Leonardo Belpassi,[b] Fabio Marchetti[a]*

[a] Università degli Studi di Pisa, Dipartimento di Chimica e Chimica Industriale, via Giuseppe Moruzzi, 13 - 56124 Pisa, Italy

[b] Istituto di Scienze e Tecnologie Molecolari del CNR (CNR-ISTM), c/o Dipartimento di Chimica, Biologia e Biotecnologie, Università degli Studi di Perugia, via Elce di Sotto 8, I-06123 Perugia, Italy

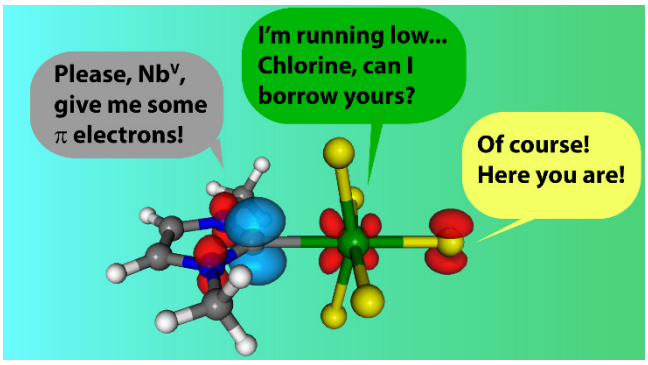

ABSTRACT

In the last years, some N-Heterocyclic Carbene complexes of high valent d^0 transition metal halides have been structurally characterized, showing a significant short distance between the carbene carbon and the *cis*-halide ligands (Cl_{ax}). Some authors attributed this arrangement to a halide → $C_{carbene}$ "back-donation", whereas, according to others, the M-carbene bond is purely σ. More in general, the ability of d^0 metal centers to provide back-donation to suitable ligands is still debated, and detailed bond analyses for this class of systems are missing in the literature. In this contribution, we analyze in detail the Nb^V-L bond within neutral, cationic and anionic derivatives of $NbCl_5$, with L = NHC carbene, CO, CNH and CN. We conclude that the d^0 niobium center is able to back-donate to L, especially in the presence of a good electron-donating group (e. g. chloride) in *trans*

position. In [$Nb^{V}Cl_5$(NHC)] complexes, with NHC being either a model carbene (1,3-dimethyl-imidazol-2-ylidene, IMe) or a realistic one (IPr), we demonstrate that the metal centre is really capable of back-donation to the carbene ligand by a charge flux that involves the Cl in *trans* position and, directly, the metal. In this case a direct interaction between Cl_{ax} and $C_{carbene}$ can be excluded, while if different π acceptor ligands, such as CO or CNH, are used (instead of NHC), the direct $Cl_{ax} \rightarrow$ L interaction is the main contribution to the π back-donation.

INTRODUCTION

Since the introduction of the Dewar-Chatt-Duncanson (DCD) model,[1] which almost 70 years ago proposed an elegant framework to rationalize the coordination of an alkene to a transition metal (M), inorganic chemists expanded this concept to the coordination of a variety of ligands (L), including carbon monoxide, [2] phosphines[3] and carbenes,[4] and demonstrated its general applicability. According to the DCD model, the M-L bond can be decomposed into two components, a L → M σ donation and M → L π back-donation. Unfortunately, the correct partitioning of the bond is not always straight-forward, since other factors, as the polarization of the ligand, should be taken into account. For example, in the case of the M-CO bonding, π back-donation transfers electronic density from the filled *d* orbitals of the metal to the π* orbital of the carbonyl, weakening the C-O bond and, consequently, causing a red-shift of the C-O stretching frequency (υ_{CO}) in the IR spectrum. This feature led to the definition of the well-known "Tolman Electronic Parameter", which is a methodology aimed to evaluate the electron-donating properties of L through the IR spectrum of [$LNi(CO)_3$] complexes.[5] On the other hand, carbonyl complexes that exhibit a blue-shift of υ_{CO}, called "nonclassical" or "abnormal",[6] were initially believed to receive no back-donation, but this supposition has been now completely overcome. Indeed, υ_{CO} is univocally determined by the direction of the CO bond polarization, with the π back-donation favoring the C → O polarization, and the electrostatic influence of the metal, whose effect depend on the net charge and the electronic distribution on the metal fragment. In this framework, it is now clear that

a blue shift does not imply negligible π back-donation, otherwise the metal fragment induces a C ← O polarization that outweighs the π effect.[7]

Particularly interesting is the bonding in d^0 metal complexes: in principle, the metal centers should not be able to back-donate electronic density to the ligand because their *d* orbitals are formally empty, but the situation is reasonably more complex. For example, the d^0 metal complexes $[Cp^*_2M(H)_2(CO)]$ ($M = Zr^{IV}$, Hf^{IV}) exhibit a classical behavior (υ_{CO} = 2044 and 2036 cm^{-1} for Zr and Hf, respectively[8]), and it has been proposed that "back-donation" could come from a M-H orbital of appropriate symmetry.[9]

The presence of both L → M σ donation and M → L π back-donation, the latter providing some contribution to the bonding, has been recognized and widely accepted also in transition metal-NHC complexes.[10]

Somehow resembling carbon monoxide,[11] NHC carbenes are basically not suitable ligands to high valent metal species.[12] Nevertheless, with reference to high valent transition metal halides with the metal in its highest oxidation state (HVTM; oxidation state of the metal > 4, d^0 configuration), a restricted number of NHC complexes have been recently reported and structurally characterized, i.e. $[VOCl_3(IMes)]$ (IMes = 1,3-dimesitylimidazol-2-ylidene),[13] $[NbCl_5(IPr)]$ (IPr = 1,3-bis(2,6-diisopropyl-phenyl)imidazol-2-ylidene),[14] $[TaBr_5(IPr)]$,[15] $[TaCl_5(NHC)]$,[16] $[MCl_4(NHC)_2][MCl_6]$ (M = Nb, Ta, NHC = N-Heterocycle Carbene = IPr or IMes),[16] $[NbOF_3(IPr)]_2$ [17] and $[WO_2Cl_2(IPr)]$.[18] All of the chloride complexes exhibit a peculiar structural arrangement: the chlorides *cis* to the carbene, forming a plane almost perpendicular to the NHC ring (Cl_{ax}), are slightly bent toward the carbene itself, the angle $C_{carbene}$-M-Cl_{ax} ranging from 81.84° to 85.09° for $[NbCl_4(IPr)_2]^+$ and $[TaCl_4(IMes)_2]^+$. Furthermore, the distance $C_{carbene}$-Cl_{ax} is generally shorter than the sum of the van der Waals radii of the two atoms. These aspects led some authors to propose a $Cl_{ax} \rightarrow C_{carbene}$ interaction (or M-$Cl_{ax} \rightarrow C_{carbene}$),[13] playing the role of unusual back-donation, similarly to what mentioned above for the Zr-H → CO case. The same kind of suspected interaction between a NHC carbene and *cis*-chloride ligand was observed also for Ti^{IV} [19] and Re^{V} [20]complexes.

In the former case, it was explained with an orbital overlapping between chloride lone pairs and the vacant C(*2p*) orbital of the carbene. In other papers, the Nb-carbene bond was described as purely σ.[14,15]

An ideal tool to study this controversial topic is the Charge Displacement (CD)[21] analysis, which has recently demonstrated its potential in the detailed and quantitative characterization of coordinative bonds,[7b,c,22] and as a useful tool to relate donation/back-donation components to experimental properties.[23]

The [$NbCl_5$(IPr)] complex represents an interesting starting point for such a study: it displays one of the longest Nb-C bonds ever reported,[14] this feature being possibly ascribable to weak bonding as well as the steric demand exerted by four *cis*-chloride ligands (note that *e.g.* [$VOCl_3$(IMes)] and [WO_2Cl_2(IPr)] contain only three chlorides adjacent to the NHC moiety).

In this paper, we applied the CD to [$NbCl_5$(NHC)] complexes (Scheme 1), with NHC being either a model carbene (1,3-dimethyl-imidazol-2-ylidene, IMe) or a realistic one (IPr), in order to clarify i) if the metal centre is really capable of back-donation to the carbene ligand, ii) if a real interaction occurs between Cl_{ax} and $C_{carbene}$ and iii) whether such interaction, if any, can be recognized as a π back-donation.

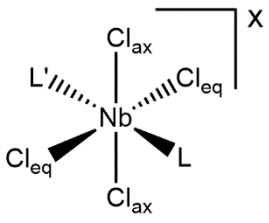

1: L = IMe; L' = Cl; x = 0
2: L = IPr; L' = Cl; x = 0
3: L = L' = IPr; ; x = +1
4: L = CO; L' = Cl; x = 0
5: L = CNH; L' = Cl; x = 0
6: L = CN; L' = Cl; x = -1

Scheme 1. Numbering of the complexes studied here.

A series of model ligands with different σ donation/π back-donation properties (carbon monoxide, cyanide, hydrogen isocyanide, see Scheme 1) have been considered, too, in order to verify the possibility of generalizing the finding concerning [$NbCl_5$(NHC)].

According to the results presented here, the [$NbCl_5$(NHC)] niobium center, despite its formal d^0 configuration, can back-donate electronic density to the carbene, while there is no direct flux between Cl_{ax} and $C_{carbene}$. On the other hand, this result is not general, since such a direct transfer becomes possible when NHC is formally replaced with carbon monoxide or a isonitrile.

COMPUTATIONAL DETAILS

All geometry optimizations have been computed with the ADF package (version 2012.01)[24] at DFT level using TZ2P Slater-type basis sets, Becke's exchange functional[25] in combination with the Lee–Yang–Parr correlation functional,[26] frozen core approximation (1s for N, C and O, 2p for Cl and 3d for Nb) and ZORA Hamiltonian to account for scalar relativistic effects.[27] We employed the numerical integration grid with precision 6.0. Electron densities used for the bond analysis (Charge-Displacement Energy Decomposition Analysis) have been computed with the version 2014.09. All the studied geometries that have been optimized are local minima, as confirmed by frequencies analysis.

Charge Displacement Analysis. The Charge Displacement analysis is based on Eq. 1. $\Delta\rho(x,y,z)$ is the difference between the electron density of a complex and that of its noninteracting fragments placed in the same position as they occupy in the complex. In the present case, the fragments are $[NbCl_{5-x}(L_x)]^{+x}$ and $L^{-1/0}$ (Scheme 1). The function $\Delta q(z)$ defines, at each point z along a chosen axis, the amount of electron charge that, upon formation of the bond between the fragments, moves across a plane perpendicular to the axis through the point z. A positive (negative) value corresponds to electrons flowing in the direction of decreasing (increasing) z. Charge accumulates where the slope of Δq is positive and decreases where it is negative.

$$\Delta q(z') = \int_{-\infty}^{+\infty} dx \int_{-\infty}^{+\infty} dy \int_{-\infty}^{z'} dz \Delta\rho(x,y,z) \qquad \text{Eq. 1}$$

The systems studied herein have C_{2v} symmetry and the z axis was chosen to coincide with the symmetry axis that passes through the niobium and the atom of L directly coordinated to the metal. This permits the separation of the $\Delta\rho$ function in components according to Eq.2 and 3, in which p represents the four irreducible representations A_1, A_2, B_1 and B_2. AB, A, and B represent the complex and its two fragments, respectively, and ϕ_i are the Kohn–Sham orbitals. This originates a separate CD function for each symmetry in each complex.[28] We define the molecular plane (σ_h) as that containing the metal center and the two equatorial chlorides (Cl_{eq}). When L = NHC, σ_h contains also the plane of the carbene.

$$\Delta\rho = \sum_p \Delta\rho_p \qquad \text{Eq. 2}$$

$$\Delta\rho_p = \sum_{i\epsilon p}\left|\phi_i^{(AB)}\right|^2 - \sum_{i\epsilon p}\left|\phi_i^{(A)}\right|^2 - \sum_{i\epsilon p}\left|\phi_i^{(B)}\right|^2 \qquad \text{Eq. 3}$$

In order to extract a CT value from the Δq curve, it is useful to fix a plausible boundary separating the fragments in the adducts. Unless otherwise specified, we chose the isodensity value representing the point on the z axis at which equal-valued isodensity surfaces of the isolated fragments are tangent. At this point, the value of Δq is represented by CT.

Energy Decomposition Analysis. To gain insights into the Nb−L bond, we carried out energy decomposition analysis (EDA)[29] as implemented in the ADF package. This method allows the decomposition of the bond energy into contributions associated with the orbital, Pauli, and electrostatic interactions. The interaction energy between two fragments is divided into three terms, as shown in Eq. 4:

$$\Delta E_{int} = \Delta E_{elst} + \Delta E_{Pauli} + \Delta E_{oi} = \Delta E^0 + \Delta E_{oi} \qquad \text{Eq. 4}$$

ΔE_{elst} is the classical electrostatic interaction between the unperturbed charge distributions of the fragments (ρ_A and ρ_B) at their final positions in the adduct. The Pauli repulsion (ΔE_{Pauli}) arises as the energy change associated with going from $\rho_A + \rho_B$ to the antisymmetrized and renormalized wave function, thus properly obeying the Pauli principle, and it comprises the destabilizing interactions between the occupied orbitals and is responsible for any steric repulsion. The last term, ΔE_{oi}, is the contribution arising from allowing the wave function to relax to the fully converged one, accounting for electron pair bonding, charge transfer, and polarization. The sum of the electrostatic interaction ΔE_{elst} and ΔE_{Pauli}, ΔE^0, is usually called the steric interaction energy.

RESULTS AND DISCUSSION

The model complex **1** bears a carbene with a small steric hindrance, which does not prevent the rotation around the Nb-$C_{carbene}$ bond. For this, in the lowest energy minimum (**1min**), the plane of the carbene is 45° tilted with respect to the chlorides (Figure 1), thus becoming all equivalent to each other. Even if in the realistic complex, **2**, the steric hindrance of the carbene does not allow this arrangement and the plane of the carbene is almost co-planar to two chlorides (experimental dihedral N-$C_{carbene}$-Nb-Cl_{eq} angle = -1.66),[14] **1min** is a good starting point for our study. Notably, also in the geometry of **1min** the chlorides in *cis* position are bent toward the carbene, with a $C_{carbene}$-Nb-Cl $_{angle}$ of 86.2°.

Firstly, it is interesting to analyze the maps associated with the different components of $\Delta\rho(x,y,z)$, which qualitatively describe the electronic deformation upon the formation of the Nb-L bond. For **1min**, we can see in Figure 1 that in the A_1 components there is a depletion of electronic density on $C_{carbene}$, an accumulation in the region between L and the metallic fragment and on the metal itself. Moreover, an accumulation of charge density is also present on the chlorides. For the chloride in *trans* position to the NHC (Cl_{trans}), the accumulation seems more pronounced and localized on the p_z orbital involved in the Nb-Cl bond, whereas for the other chlorides, the accumulation recalls the shape of the p_z orbital perpendicular to the Nb-Cl bond (lone pair). The carbene backbone exhibits a

depletion/accumulation pattern typical of the polarization.[22b] The A_1 component is clearly associated with the L → M σ donation.

The A_2 components is associated only with a small polarization of the two fragments and cannot be associated to any bond component.

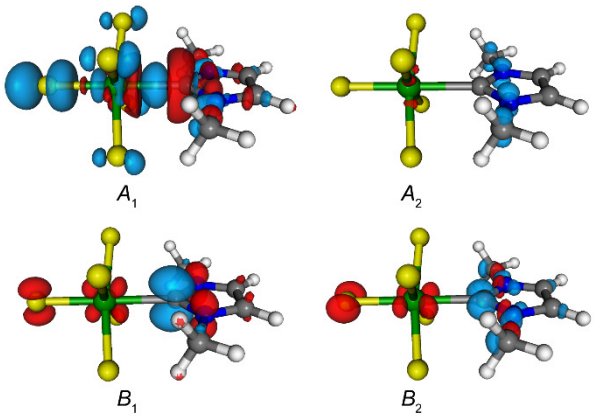

Figure 1. Isodensity surfaces (±0.0015 e/a.u) for the A_1, A_2, B_1 and B_2 components of $\Delta\rho(x,y,z)$ for complex **1min**.

The B_1 component exhibits an accumulation on $C_{carbene}$ and a depletion on the niobium and on Cl_{trans}. The shape of the regions closely recalls the empty p_y orbital of the carbene as acceptor and the p_y orbital of one lone pair of Cl_{trans} and the *d* orbitals of the metal as donors. The B_1 component can be related with the out-of-plane M → L π back-donation, whereas the depletion region on Cl_{trans} indicates that the latter is likely the primary source of electrons for the back-donation. Noteworthy, if a lower threshold is used (see Figure S1, Supporting Information), the depletion region on the metal clearly involves all the four Nb-Cl bonds. The other chlorides do not present a depletion region and, therefore, are not involved at all in the back-donation process. On the contrary, lowering the threshold value, small accumulation regions appear (see Figure S1, Supporting Information).

Finally, in the B_2 component there is an accumulation on the $C_{carbene}$-N bond and a depletion on the metal and on Cl_{trans}. As described also for the Au-carbene bond,[22b] this component describes the in-plane M → L π back-donation.

Now, it is possible to quantify the different electronic fluxes, integrating $\Delta\rho(x,y,z)$ on the Nb-$C_{carbene}$ axis. The corresponding CD curves are shown in Figure 2.

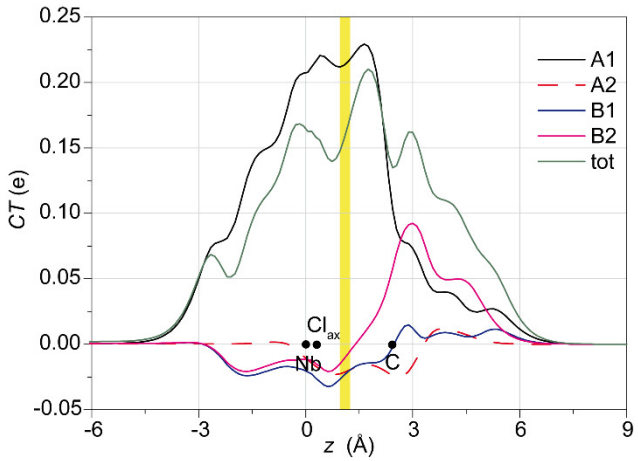

Figure 2. Total CD curve and its symmetry components for the Nb–$C_{carbene}$ bond in the complex **1min**. Black dots indicate the *z* position of the atomic nuclei. A yellow vertical band indicates the boundary (see Computational Details) between the [$NbCl_5$] and the IMe fragments.

As a result of the integration, the values of the CD curves at the isoboundary, indicated as CT(A_1), CT(A_2), CT(B_1) and CT(B_2), can be quantified as 0.213, -0.021, -0.023 and -0.009 e, respectively. The total charge flux, CT(tot), is 0.162 e (L → M direction). The B_1 curve is negative throughout all the metallic fragment and also in the inter-fragments region, indicating a real charge transfer from the metal fragment to the carbene. The shape of the curve confirms that Cl_{trans} is an important source of electrons for the back-donation: comparing the values of Δq between Cl_{trans} and Nb (-0.021 e), and between Nb and $C_{carbene}$ (-0.023 e), it emerges that Cl_{trans} provides almost all the electronic density back-donated to IMe. The same curve becomes positive in the carbene region because of the ligand polarization induced from the metal fragment. The B_2 curve has a similar shape, but the carbene polarization is much more intense.

We can now focus on the higher energy minimum **1** (ΔE = +5.1 kcal/mol with respect to **1min**) with the dihedral N-$C_{carbene}$-Nb-Cl_{eq} angle set to zero, which is closer to the realistic complex **2**.

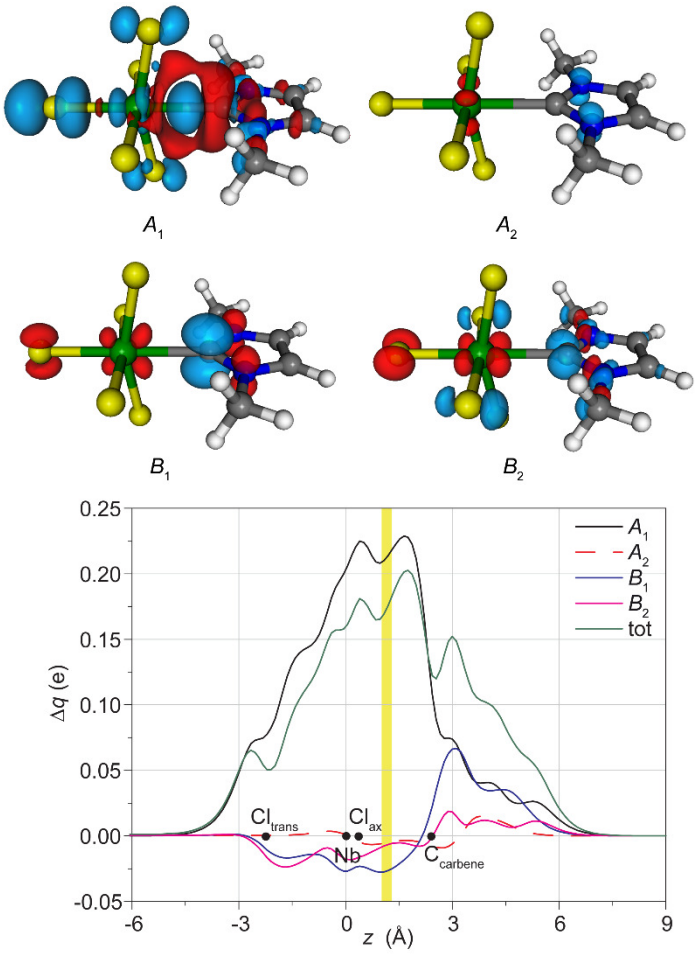

Figure 3. Up: isodensity surfaces (±0.0015 e/a.u.) for the A_1, A_2, B_1 and B_2 components of $\Delta\rho(x,y,z)$ for **1**. Down: total CD curve and its symmetry components for the Nb–$C_{carbene}$ bond in the complex **1**. Black dots indicate the z position of the atomic nuclei. A yellow vertical band indicates the boundary (see Computational Details) between the [$NbCl_5$] and the IMe fragments.

The situation is very similar to that discussed for **1min**, with the difference that in this case the depletion on the metal in the B_1 component involves only the chlorides perpendicular to the plane of the carbene (Cl_{ax}, see Figure 3). In this case, the integration of the A_1, A_2, B_1 and B_2 CD curves at the isoboundary can be quantified as 0.214, -0.005, -0.026 and -0.006 e, respectively, while CT(tot) is 0.178 e. Interestingly, the sum of the two back-donation components, B_1 and B_2, is the same for **1min** and **1** (-0.032 e), but for the latter the B_1 component is larger and the B_2 is lower. This is likely

due to the different degree of overlapping between the *d* orbitals of the metal and the p_y orbital of the NHC, which is more effective when the two orbitals are parallel. No direct $Cl_{ax} \rightarrow C_{carbene}$ interaction is visible and the chlorides present an accumulation region rather than a depletion.

Before passing to the description of a more realistic system, it is interesting to analyze more in detail the charge accumulation mentioned above on the chlorides. This is mainly due to a significant polarization of the Cl-Nb bonds, with a charge shift from the Nb to Cl_{ax}, in response of the approaching of the electron-rich $C_{carbene}$. The nature of a such polarization is probably of electrostatic nature, as a very similar pattern of polarization on the metal fragment is induced substituting the ligand with a negative charge (Figure S2, Supporting Information), and is not related to the Nb-NHC bond components.

Now, in this framework, we can analyze the realistic system **2**, in which the optimized geometry is the lowest energy minimum and very close to the X-ray structure. In the latter, the N-$C_{carbene}$-Nb-Cl_{eq} dihedral angle is -1.66°,[14] whereas in the C_{2v} optimized structure it is obviously 0°, but such deviation is negligible.

The electronic situation in **2** is very similar to those in **1** (Figure 4). A large σ-donation with the strong polarization of the Nb-Cl_{trans} bond in the A_1 symmetry (CT(A_1) = 0.204 e), a negligible polarization in the A_2 symmetry (CT(A_2) = -0.012 e), an electronic flux that start from the p_y orbital of Cl_{trans}, passes through the d^0 orbital of Nb and accumulates on the p_y orbital of the carbene in the B_1 symmetry (CT(B_1) = -0.031 e), and, finally, an electronic flux that start from the p_x orbital of Cl_{trans}, passes through the d^0 orbital of Nb and accumulates on the C-N orbital of the carbene in the B_2 symmetry (CT(B_2) = -0.005 e). The sum of all these components, CT(tot) is 0.156 e.

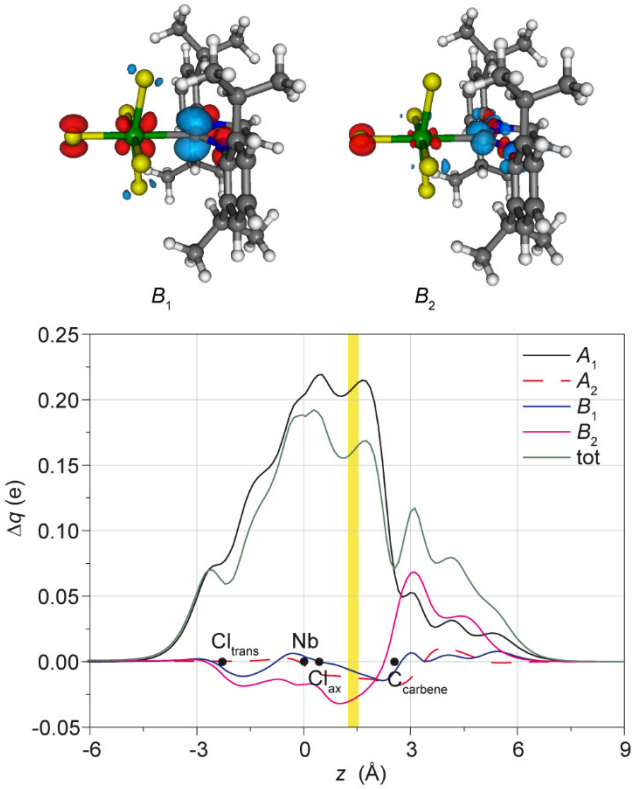

Figure 4. Up: Isodensity surfaces (±0.0015 e/a.u.) for the B_1 and B_2 components of $\Delta\rho(x,y,z)$ for **2** (A_1 and A_2 components can be found in the Supporting Information). Down: Total CD curve and its symmetry components for the Nb–$C_{carbene}$ bond in the complex **2**. Black dots indicate the *z* position of the atomic nuclei. A yellow vertical band indicates the boundary (see Computational Details) between the [$NbCl_5$] and the IPr fragments.

Also in this case, no direct electronic displacement from the chlorides to the carbene can be noted. The next step is to investigate the possibility of back-donation in d^0 cationic complexes, which intuitively seems even more unlikely than in the case of neutral systems. We chose to study the cationic *bis*-carbene $[NbCl_4(IPr)_2]^+$ (**3**) that has been structurally characterized.[16] As in the experimental structure, the two carbene are perpendicular to each other and the chlorides are bent toward the carbene with respect to which they are perpendicular. Our geometry is constrained to a C_{2v} symmetry, whereas in the experimental structure the dihedral angles N-$C_{carbene}$-Nb-Cl_{eq} go from -3.68 to 25.06 degrees.[16]

Considering the fragments $[NbCl_4(IPr)]^+$ and IPr, the most relevant deformation density maps are showed in Figure 5. Notably, both in-plane and out-of-plane back-donation components are still clearly visible. In both cases, the carbene belonging to the metallic fragment is depopulated, analogously to the depletion on Cl_{trans} already seen in complexes **1** and **2**.

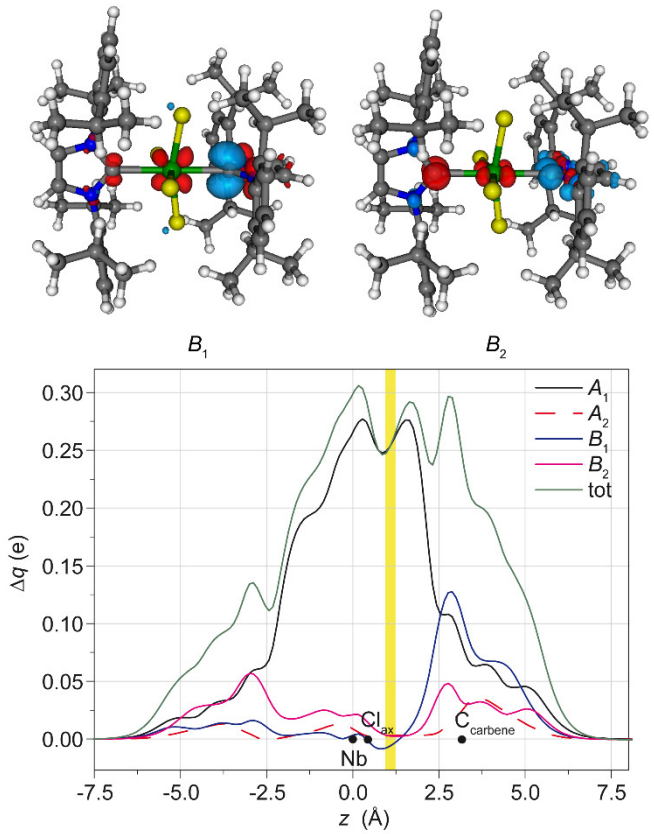

Figure 5. Up: Isodensity surfaces (±0.0015 e/a.u.) for the B_1 and B_2 components of $\Delta\rho(x,y,z)$ (A_1 and A_2 components can be found in the Supporting Information) for **3**. Down: Total CD curve and its symmetry components for the Nb–$C_{carbene}$ bond in the complex **3**. Black dots indicate the *z* position of the atomic nuclei. A yellow vertical band indicates the boundary (see Computational Details) between the $[NbCl(IPr)]^+$ and the IPr fragments.

Quantifying the components, CT(A_1), CT(A_2), CT(B_1) and CT(B_2), are 0.260, 0.003, -0.003 and 0.002 e, respectively. In this case, the back-donation is indeed very low, as it could be expected, but

it can be noted that the polarization at $C_{carbene}$ is much more intense than in the case of **2**, 0.127 and 0.068 e, respectively, which makes more difficult the exact quantification of back-donation. The depletion regions on the carbene of the metallic fragment in the B_1/B_2 components are analogous to those present on Cl_{trans} for **1min**, **1** and **2**, making us think that the back-donation is small only because the carbene is a weak electron-donating group. But, again, the chlorides, despite their arrangement, do not interact at all with $C_{carbene}$.

It is now interesting to see if the results here presented for carbenes ligands can be generalized to other ligand with different donation/back-donation properties. The archetypical ligand to study M → L π back-donation is obviously the carbon monoxide. The carbonyl complex $[NbCl_5(CO)]$ (**4**) has not been synthesized, but it can be theoretically modeled. In this case, all the chlorides are equivalent and all of them are bent toward the carbonyl moiety (C_{CO}-Nb-Cl angle = 80.6°). The Nb-Cl_{trans} bond is 2.298 Å, considerably shorter than in the case of **1** (2.370 Å, see below).

The stretching frequency of the carbonyl, υ_{CO}, is 2136 cm^{-1}, which is slightly higher than the value for the free CO calculated with the same theory level (2106 cm^{-1}), making the complex, unsurprisingly, "nonclassical". The interaction energy of the Nb-CO bond, which is only -4.87 kcal/mol, gives a likely explanation about why **4** has never been isolated. The low value is mainly due to the fact that the electrostatic component of the bond (-48.8 kcal/mol, see Table S1, Supporting Information) is not negative enough to compensate the repulsive Pauli component (77.8 kcal/mol). In the case of **1**, for instance, the two values are more similar, in absolute value (-89.4 and 97.5 kcal/mol, respectively, Table S1). However, in spite of the low total interaction energy, the stabilizing orbital term is significant (-33.9 kcal/mol) and is only slightly smaller than that of the systems bearing NHC ligands (-43.8 and -44.6 kcal/mol for **1** and **2**, respectively).

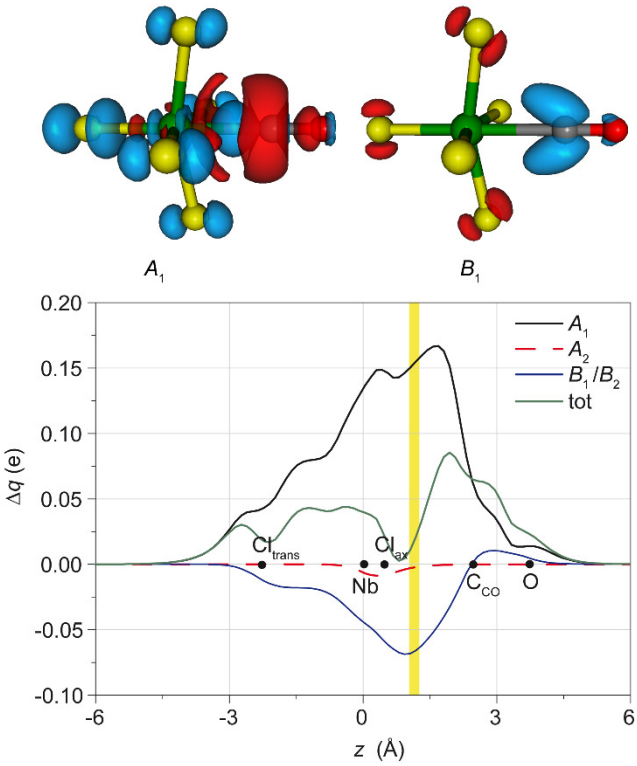

Figure 6. Isodensity surfaces (±0.0015 e/a.u.) for the A_1 and B_1 $\Delta\rho$(x,y,z) (the B_2 component is identical to B_1, A_2 is a non-relevant polarization analogously than before) of **4**. Down: Total CD curve and its symmetry components for the Nb–C_{CO} bond in the complex **4**. Black dots indicate the *z* position of the atomic nuclei. A yellow vertical band indicates the boundary (see Computational Details) between the [$NbCl_5$] and the CO fragments.

For the A_1 component, the situation for **4** is similar than in the case of **1** (depletion on C_{CO}, accumulation between C_{CO} and Nb, polarization on chlorides, Figure 5). Also the A_2 component is very similar in shape and very close to zero throughout all the complex. On the contrary, the B_1 component is surprisingly different than before, not only quantitatively, but from the qualitative point of view. A pronounced density accumulation is visible on the ligand, and the shape of the region recalls a π* orbital of the triple bond, but distorted and pointing directly toward Cl_{ax}. For the metallic fragment, only depletion regions are visible, either on the metal, with a shape resembling the *d* orbitals of the niobium (a lower isodensity value is needed for this, see Figure S5, Supporting Information), on Cl_{trans} and two Cl_{ax} out of four. Clearly, the other two Cl_{ax} show the same

deformation in the B_2 component. For the chlorides, the shapes of the depletion recall the *p* orbitals of the lone pairs, but in the case of Cl_{ax}, the shape is distorted to point directly toward C_{CO}.

The CD curves quantitatively describe the situation presented above along the z axis. The A_1 curve is always positive, indicating an electronic flux that goes from the ligand to the metal and to Cl_{trans} without any interruption. On the other hand, the B_1/B_2 curves are negative throughout all the metallic fragment and the interfragment region, but become positive in the region of the triple bond, indicating the presence of M → L back-donation but also ligand C ← O polarization. In numbers, CT(A_1), CT(A_2) and CT(B_1) are equal to 0.155, -0.002 and -0.066 e, respectively. The total back-donation, CT(B_1) + CT(B_2), consequently, is -0.132 e and the resulting CT(tot) is 0.021 e. Taking the value of Δq at the midpoint of the carbonyl bond, $CT^{\pi}_{r/2}$, the polarization of the carbonyl is quantified, as well, as 0.02 e. Just to have a benchmark, this is the same value calculated for $[(IPr)Au(CO)]^+$,[7b] for which the presence of back-donation has been demonstrated. And, indeed, for both the systems also the C-O bond distance is very similar to that for the free CO (Δr = -0.004 and -0.001 Å for **4** and $[(IPr)Au(CO)]^+$, see Figure S6, Supporting Information).

In order to understand whether the qualitative difference between the M → carbene and M → CO fluxes is due to the presence of the triple bond, the complex bearing the simplest isocyanide, CNH, and the cyanide anion, CN^-, as ligand have been studied (complexes **5** and **6**, respectively).

The optimized geometry of complex **5**, is similar to that of **4**, with C_{CNH}-Nb-Cl angle is 81.6° and Nb-Cl_{trans} = 2.316 Å. The interaction energy is -16.52 kcal/mol (Table S1). Also in this case, the electrostatic component is unfavorable, but to a lesser extent than in the case of **4**, and the orbital interaction (-35.5 kcal/mol) is similar to the systems studied before. We can now analyze the electronic deformation upon the formation of the Nb-CNH bond (Figure 7).

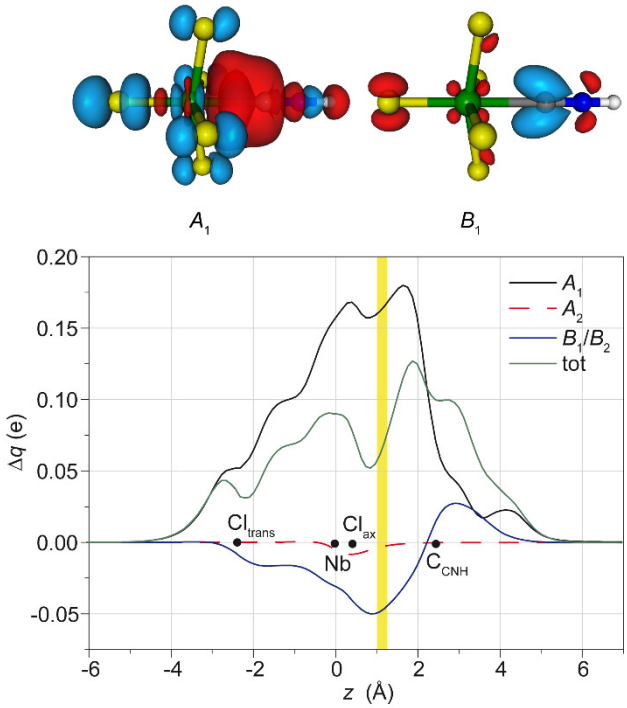

Figure 7. Up: Isodensity surfaces (±0.001 e/a.u.) for the A_1 and B_1 $\Delta\rho$(x,y,z) (the B_2 component is identical to B_1) for **5**. Down: Total CD curve and its symmetry components for the Nb–C_{CNH} bond in the complex **5**. Black dots indicate the *z* position of the atomic nuclei. A yellow vertical band indicates the boundary (see Computational Details) between the [$NbCl_5$] and the CNH fragments.

In this case, the B_1 component seems to be intermediate between **1** and **4**, with depletion regions clearly visible on both the metal and Cl_{ax} (Figure 7).

It is important to underline that the CD curves cannot discriminate between the back-donation coming from the metal or from the chlorides, since they have the same symmetry. On the other hand, the isodensity maps are essentially qualitative. Quantitatively, for **5** CT(A_1), CT(A_2), CT(B_1/B_2), are 0.166, -0.002 and -0.046 e, respectively, leading to a value for CT(tot) of 0.072 e.

The geometry of **6** is similar to that of **4** and **5**, but the Nb-Cl_{trans} distance is 2.417 Å, even longer than in **1**, and C_{CN}-Nb-Cl_{ax} = 86.3°, the largest value among all the complexes studied here. The complete bond analysis for **6** is reported in the Supporting Information (Figure S7), but we can underline here that also in this case the visual inspection of the B_1 component of $\Delta\rho$ show a small π

back-donation coming from the p_y orbital of Cl_{trans} and the *d* orbitals of the metal to the π* orbital of the ligand. No depletion region is visible on Cl_{ax} or Cl_{eq}.

Looking back to the results presented up to now, we can appreciate that the fragment [$NbCl_5$] is able to back-donate to L in two ways: through the *d* orbitals of the metal, partially filled by the chlorides and with the help of Cl_{trans} (carbenes and, to a lesser extent, CN^-) or through the p_z lone pair of $Cl_{ax/eq}$ (CO and CNH). For the ligands containing a triple bond, a likely explanation seems to rely on the different L-Nb-Cl_{ax} angle: the latter is low for CO (80.6°), favoring the overlapping between the lone pair of the chloride and the π* anti-bonding orbital of the carbonyl and making the Cl → L direct interaction the predominant one, whereas the same angle is much larger for CN^- (86.3°), due to the repulsion between the electron density of the cyanide and that of the Nb-Cl bonds, unfavouring the overlapping and leaving only the M → L interaction. For CNH, the angle is intermediate (81.6°) and the two contributions, Cl → L and M → L, are equally important. The L-Nb-Cl_{ax} angle of the complexes bearing carbene ligands cannot be directly compared to the others, since the four chlorides are not equivalent each other and the angle depends also on the steric properties of the carbene. But we expect that the empty p_y orbital of the carbene is likely much more localized than the π* of the triple bond, making the Cl → L negligible, as unambiguously demonstrated by CD.

It is interesting to notice that in all the cases studied here, Cl_{trans} undergoes a complex electronic rearrangement: an accumulation of electronic density as consequence of the Nb ← L σ donation and a depletion because of the Nb → L π back-donation. For this reason, the relationship between the Nb-Cl_{trans} bond distance and the donation/back-donation properties of L, if any, is not trivial. The most important orbital interaction between the metal, Cl_{trans} and the ligand are depicted in Figure 8 for the case of carbene. The lone pairs of Cl_{trans} and $C_{carbene}$ both interacts with the d_{z^2} orbital of the metal, forming a three center-four electrons system. According to this model, strong donating ligands should decrease the Nb-Cl_{trans} bond order, causing a lengthening of the Nb-Cl_{trans} bond. This

is qualitatively confirmed by the fact that the longest bond can be found in **6**, bearing a cyanide as ligand. On the other hand, the back-donation process can be explained using the d_{yz} orbital of the metal, which accepts electronic density from the p_y lone pair of the chloride and transfers it on the p_y empty orbital of the ligand (Figure 8). This is supported by the shape of the CD(B_1/B_2) curves, which demonstrates that most of the back-donated electronic density comes from Cl_{trans} (see before), if present. According to this vision, π accepting ligands should led to an increase of the Nb-Cl_{trans} bond order.

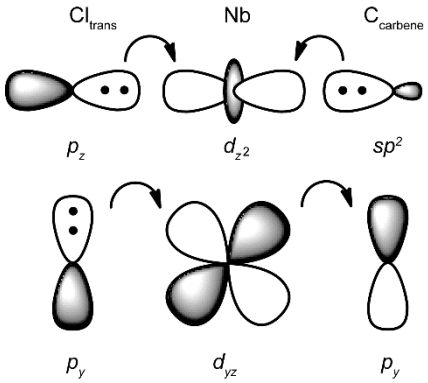

Figure 8. A stylized depiction of the most important bonding interactions involving Cl_{trans}, Nb and $C_{carbene}$.

Comparing the Nb-Cl_{trans} bond distance with the components of the Nb-L bond, it can be seen that it linearly correlates with either the total π back-donation (CT(B_1) + CT(B_2), r^2 = 0.9952), the σ donation (CT(A_1), r^2 = 0.9466) and, consequently, with the total (CT(tot), r^2 = 0.9691) (see Figure 9). Noteworthy, the Nb-Cl_{trans} bond distance is longer in the presence of strong σ-donating ligands (high values of CT(A_1)) and is shorter with strong π-acceptor ligands (high values, in absolute value, of CT(B_1/B_2)), confirming the orbital model proposed in Figure 8.

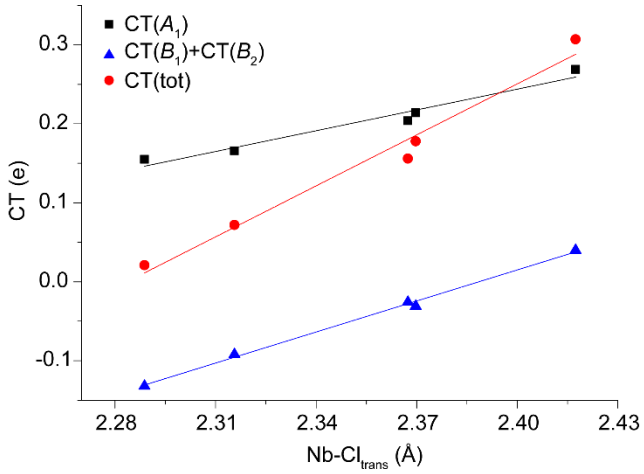

Figure 9. Correlation between Nb-Cl$_{trans}$ bond distances for complexes **1**, **2**, **4**, **5** and **6** and the corresponding bond components.

CONCLUSIONS

In this paper, we investigated in detail the bond between the [NbCl$_5$] fragment and various ligands, including the carbene IPr, whose complex has been experimentally characterized,[14] in order to establish whether a high valent d^0 metal is capable of back donation bonding, and eventually to clarify the possible role of the Cl ligands. The CD analysis, coupled with the visual inspection of deformation density maps, demonstrated that, either using a realistic or a model carbene (IMe):

1) YES, the metal can really back-donate using its *d* orbitals, which are only formally empty, mainly exploiting the electronic charge of Cl$_{trans}$; in the absence of a strong electron-donating ligand in *trans*, back-donation is much weaker, even if not null.

2) NO, the Cl$_{ax}$ are not involved in the back-donation; nonetheless, expanding the scope of the work to theoretical models, it emerges that in some cases the direct Cl$_{ax}$ → L back-donation is possible, for example substituting the carbene with carbon monoxide or an isocyanide.

Finally, the Nb-Cl$_{trans}$ bond distance and, to a lesser extent, the L-Nb-Cl$_{ax}$ angle can be used as an experimental probe for the characterization of the Nb-L bond. In this sense, the structural characterization of other Nb^V complexes is of fundamental importance to verify our predictions.

ASSOCIATED CONTENT

Additional figures, EDA results and optimized geometries.

AUTHOR INFORMATION

*GC: E-mail: gianluca.ciancaleoni@unipi.it; Orcid: orcid.org/0000-0001-5113-2351;

LB: Orcid: orcid.org/0000-0002-2888-4990;

FM: Orcid: orcid.org/0000-0002-3683-8708.

ACKNOWLEDGEMENTS

GC acknowledges the University of Pisa for financial support.

REFERENCES

[1] Dewar, M. J. S. *Bull. Soc. Chim. Fr*. **1951**, *18*, C71 – C79; Chatt, J.; Duncanson, L. A. *J. Chem. Soc*. **1953**, 2939.

[2] Crabtree, R. H. *The Organometallics Chemistry of the Transition metals*, 4th ed.; John Wiley & Sons Inc.: Hoboken, **2005**.

[3] (a) Xiao, S.-X.; Trogler, W. C.; Ellis, D. E.; Berkovitch-Yellin, Z. *J. Am. Chem. Soc*. **1983**, *105*, 7033; (b) Tossell, J. A.; Moore, J. H.; Giordan, J. C. *Inorg. Chem*. **1985**, *24*, 1100; (c) Rolke, J.; Brion, C. E. *Chem. Phys*. **1996**, *207*, 173.

[4] (a) Nelson, D. J.; Nolan, S. P. *Chem. Soc. Rev.* **2013**, *42*, 6723−6753; (b) Comas-Vives, A.; Harvey, J. N. *Eur. J. Inorg. Chem*. **2011**, *2011*, 5025−5035.

[5] Tolman, C. A. *Chem. Rev*. **1977**, *77*, 313.

[6] Lupinetti, A. J.; Frenking, G.; Strauss, S. H., *Angew. Chem. Int. Ed.* **1998**, *37*, 2113-2116.

[7] (a) Goldman, A. S.; Krogh-Jespersen, K., *J. Am. Chem. Soc*., **1996**, *118*, 12159; (b) Bistoni, G.; Rampino, S.; Scafuri, N.; Ciancaleoni, G.; Zuccaccia, D.; Belpassi, L.; Tarantelli, F., *Chem. Sci.* **2016**, *7*, 1174; (c) Ciancaleoni, G.; Scafuri, N.; Bistoni, G.; Macchioni, A.; Tarantelli, F.; Zuccaccia, D.; Belpassi, L., *Inorg. Chem.* **2014**, *53*, 9907-9916.

[8] (a) Manriquez, J. M.; McAlister, D. R.; Sanner, R. D.; Bercaw., J. E. *J. Am. Chem. Soc.* **1976***, 98*, 6733; (b) Marsella, J. A.; Curtis, J. C.; Bercaw, J. E.; Caulton, K. G. *J. Am. Chem. Soc.* **1980**, *102*, 7244. (c) Roddick, D. M.; Fryzuk, M. D.; Seidler, P. F.; Hillhouse, G. L.; Bercaw, J. E. *Organometallics* **1985**, *4*, 97.

[9] (a) Lauher J. W.; Hoffman, R. *J. Am. Chem. Soc*. **1976**, *98*, 1729; (b) Brintzinger. H. H. *J. Organomet. Chem.* **1979**, *171*, 337.

[10] Nelson, D. J.; Nolan, S. P. *Chem. Soc. Rev.* **2013**, *42*, 6723.

[11] (a) Srivastava, S. C.; Shrimal, A. K. *Polyhedron* **1988**, *18*, 1639; for Nb(I) see: (b) Carnahan, E. M.; Rardin, R. L.; Bott, S. G.; Lippard, S. J. *Inorg. Chem.* **1992**, *31*, 5193 and (c) Pandey, K. K.; Tiwari, P.; Patidar, P. *J. Organomet. Chem.* **2013**, *740*, 135.

[12] Bellemin-Laponnaz, S.; Dagorne, S. *Chem. Rev.* **2014**, *114*, 8747; Bortoluzzi, M.; Ferretti, E.; Marchetti, F.; Pampaloni, G.; Pinzino, C.; Zacchini, S. *Inorg. Chem.* **2016**, *55*, 4173.

[13] Abernethy, C. D.; Codd, G. M.; Spicer, M. D.; Taylor, M. K. *J. Am. Chem. Soc.* **2003**, *125*, 1128-1129.

[14] Bortoluzzi, M.; Ferretti, E.; Marchetti, F.; Pampaloni, G.; Zacchini, S. *Chem. Commun.* **2014**, *50*, 4472-4474.

[15] Bortoluzzi, M.; Ferretti, E.; Marchetti, F.; Pampaloni, G.; Zacchini, S. *Dalton Trans.* **2016**, *45*, 6939-6948.

[16] Wei, Z.; Zhang, W.; Luo, G.; Xu, F.; Mei, Y.; Cai, H. *New J. Chem.* **2016**, *40*, 6270-6275.

[17] Bortoluzzi, M.; Ferretti, E.; Marchetti, F.; Pampaloni, G.; Zacchini, S. *J. Coord. Chem.* **2016**, *69*, 2766-2774.

[18] Dodds, C. A.; Spicer, M. D.; Tuttle, T. *Organometallics*, **2011**, *30*, 6262.

[19] Shukla, P.; Johnson, J. A.; Vidovic, D.; Cowleya, A. H.; Abernethy, C. D. *Chem. Commun.* **2004**, 360-361.

[20] Braband, H.; Abram, U. *Chem. Commun.* **2003**, 2436-2437.

[21] (a) Belpassi, L.; Infante, I.; Tarantelli, F.; Visscher, L. *J. Am. Chem. Soc.* **2008**, *130*, 1048; (b) Bistoni, G.; Belpassi, L.; Tarantelli, F. *J. Chem. Theory Comput*., **2016**, *12*, 1236–1244.

[22] (a) Gaggioli, C. A.; Bistoni, G.; Ciancaleoni, G.; Tarantelli, F.; Belpassi, L.; Belanzoni, P. *Chem. Eur. J.* DOI: 10.1002/chem.201700638; (b) Marchione, D.; Belpassi, L.; Bistoni, G.; Macchioni, A.; Tarantelli, F.; Zuccaccia, D. *Organometallics* **2014**, *33*, 4200–4208; (c) Gaggioli, C. A.; Belpassi, L.; Tarantelli, F.; Belanzoni, P. *Chem. Commun.* **2017**, *53*, 1603-1606.

[23] (a) Biasiolo, L.; Belpassi, L.; Gaggioli, C. A.; Macchioni, A.; Tarantelli, F.; Ciancaleoni, G.; Zuccaccia, D. *Organometallics* **2016**, *35*, 595-604; (b) Gaggioli, C. A.; Ciancaleoni, G.; Zuccaccia, D.; Bistoni, G.; Belpassi, L.; Tarantelli, F. **2016**, *35*, 2275-2285; (c) Ciancaleoni, G.; Biasiolo, L.; Bistoni, G.; Macchioni, A.; Tarantelli, F.; Zuccaccia, D.; Belpassi, L. *Chem. Eur. J.* **2015**, *21*, 2467-2473; (d) Marchione, D.; Izquierdo, M. A.; Bistoni, G.; Havenith, R. W. A.; Macchioni, A.; Zuccaccia, D.; Tarantelli, F.; Belpassi, L. *Chem. Eur. J.* **2017**, *23*, 2722-2728.

[24] SCM, Theoretical Chemistry, Vrije Universiteit, Amsterdam, 2008, http://www.scm.com.

[25] Becke, A. D. *Phys. Rev. A* **1988**, *38*, 3098–3100.

[26] Lee, C.; Yang, W.; Parr, R. G. *Phys. Rev. B* **1988**, *37*, 785–789.

[27] (a) van Lenthe, E.; Baerends, E. J.; Snijders, J. G. *J. Chem. Phys*. **1993**, *99*, 4597–4610; (b) van Lenthe, E.; Baerends, E. J.; Snijders, J. G. *J. Chem. Phys* **1994**, *101*, 9783–9792; (c) van Lenthe, E.; Ehlers, A.; Baerends, E. J. *J. Chem. Phys*. **1999**, *110*, 8943–8953.

[28] Salvi, N.; Belpassi, L.; Tarantelli, F. *Chem. Eur. J*. **2010**, *16*, 7231-7240.

[29] (a) von Hopffgarten, M.; Frenking, G. *WIREs Comput. Mol. Sci*. **2012**, *2*, 43−62. (b) Morokuma, K. *J. Chem. Phys.* **1971**, *55*, 1236−1244. (c) Ziegler, T.; Rauk, A. *Theor. Chim. Acta* **1977**, *46*, 1−10.